Electron Tomography Reveals Posttranscriptional Binding of Pre-mRNPs to Specific Fibers in the Nucleoplasm

Francesc Miralles,* Lars-Göran Öfverstedt,‡ Nafiseh Sabri,* Youssef Aissouni,§ Ulf Hellman,‖ Ulf Skoglund,‡ and Neus Visa*

*Department of Molecular Genome Research, Stockholm University, SE-106 91 Stockholm, Sweden; ‡Department of Cell and Molecular Biology, Karolinska Institute, SE-171 77 Stockholm, Sweden; §Institut Paoli Calmettes, INSERM-U119, Cancérologie Expérimentale, F-13009 Marseille, France; and ‖Ludwig Institute for Cancer Research, SE-751 24 Uppsala, Sweden

Abstract. Using electron tomography, we have analyzed whether the Balbiani ring (BR) pre-mRNP particles in transit from the gene to the nuclear pore complex (NPC) are bound to any structure that could impair free diffusion through the nucleoplasm. We show that one-third of the BR particles are in contact with thin connecting fibers (CFs), which in some cases merge into large fibrogranular clusters. The CFs have a specific protein composition different from that of BR particles, as shown by immuno-EM. Moreover, we have identified hrp65 as one of the protein components of the CFs. The sequencing of hrp65 cDNA reveals similarities with hnRNP proteins and splicing factors. However, hrp65 is likely to have a different function because it does not bind to nascent pre-mRNA and is not part of the pre-mRNP itself. Taken together, our observations indicate that pre-mRNPs are not always freely diffusible in the nucleoplasm but interact with fibers of specific structure and composition, which implies that some of the posttranscriptional events that the pre-mRNPs undergo before reaching the NPC occur in a bound state.

Key words: pre-mRNA • Balbiani ring particle • hrp65 • mRNA export • nuclear substructure

Introduction

Gene expression in eukaryotes involves both nuclear and cytoplasmic events. Messenger RNA precursors (pre-mRNAs) are cotranscriptionally associated with hnRNP proteins (reviewed by Krecic and Swanson, 1999) and assembled into ribonucleoprotein complexes (pre-mRNPs) that are processed in the nucleus and exported to the cytoplasm where they direct protein synthesis. Transport of pre-mRNPs from the nucleus to the cytoplasm is an active, signal-mediated process that can be subdivided into two steps: (a) intranuclear transport from the sites of transcription to the nuclear envelope, and (b) translocation through the nuclear pore complexes (NPCs)[1]. In recent years, many of the signals, adapters, and receptors involved in RNA export have been identified (reviewed by Mattaj and Englmeier, 1998). In the case of pre-mRNA, it has been shown that certain hnRNP proteins, such as hnRNP A1, carry nuclear export signals that confer bidirectional transport across the nuclear envelope (Michael et al., 1995; Izaurralde et al., 1997). However, the mechanistic aspects of pre-mRNA export remain to be elucidated. In the most simple model, the newly synthesized pre-mRNPs would be released from the chromosome upon transcription termination and diffuse through the interchromatin space (also referred to as interchromosomal channel network or nucleoplasm) to the NPCs. Meanwhile, the nuclear export signals in the protein moiety of the pre-mRNP would be recognized by soluble export receptors that would bridge the interaction between the pre-mRNP and the NPC, thus triggering translocation to the cytoplasm (for recent reviews see Mattaj and Englmeier, 1998; Stutz and Rosbash, 1998). However, it is unclear whether the transported pre-mRNPs are freely diffusible through the nucleoplasm or physically attached to nuclear structures. Both diffusion and physical attachment have found experimental support. Studies of RNA transport based on the analysis of transgenes in *Drosophila* indicated that the intranuclear movement of pre-mRNAs occurs isotropically through the interchromosomal channels at rates consistent with diffusion, and suggested that incompletely spliced pre-mRNAs are discriminated at the nuclear surface (Zachar et al., 1993). Recent kinetic studies in two independent systems

Address correspondence to Neus Visa, Department of Molecular Genome Research, Stockholm University, SE-106 91 Sweden. Tel.: 46-8-16 41 11. Fax: 46-8-16 64 88. E-mail: neus.visa@molgen.su.se

[1]*Abbreviations used in this paper:* 3D, three-dimensional; BR, Balbiani ring; CF, connecting fiber; COMET, Constrained Maximum Entropy Tomography; ET, electron tomography; FGC, fibrogranular cluster; NPC, nuclear pore complex.

have also shown that at least a large fraction of pre-mRNPs move randomly inside the nucleus at rates that are compatible with free diffusion (Politz et al., 1998; Singh et al., 1999; reviewed by Daneholt, 1999). On the other hand, rhodamine-labeled pre-mRNAs microinjected into the nucleus of living cells became localized in discrete nuclear sites rich in splicing factors, and it was shown that the localization was dependent on intron sequences (Wang et al., 1991). The hypothesis that RNA binds to nondiffusible elements was also supported by observations of pre-mRNA tracks extending towards the nuclear envelope (i.e., Xing et al., 1995), by the presence of pre-mRNA in nuclear matrix preparations (reviewed by Agutter, 1995), and by the accumulation of viral RNAs at discrete nuclear sites during intranuclear RNA transport (e.g., Bridge et al., 1996; Puvion-Dutilleul et al., 1997).

Our approach to study the possible attachment of pre-mRNAs to nucleoplasmic structures is based on the morphological analysis of endogenous pre-mRNPs in situ. We have directly visualized pre-mRNPs in transit from the gene to the nuclear envelope and asked whether the pre-mRNPs show any morphological sign of binding interactions. For this purpose we have used the salivary glands of the dipteran *Chironomus tentans* (*C. tentans*). In the nuclei of the salivary gland cells, the chromatin is confined to well-defined polytene chromosomes and thus the nucleoplasm is totally free of chromatin fibers. Moreover, in these cells the assembly, transport and disassembly of a specific pre-mRNP, the Balbiani ring (BR) particle, can be directly visualized using transmission electron microscopy (Skoglund et al., 1983). Therefore, the possible binding of pre-mRNPs to nuclear structures can be directly investigated in situ.

The BR genes encode secretory proteins and are actively expressed in the salivary gland cells in a tissue-specific manner (reviewed by Wieslander, 1994). The BR pre-mRNA is exceptionally long (35–40 kb) and is cotranscriptionally packed into a large pre-mRNP particle. The structure of the BR particle has been previously analyzed by electron tomography (ET) both in situ (Skoglund et al., 1986) and after isolation in sucrose gradients (Lönnroth et al., 1992). The BR particle can be described as a 7-nm RNP fiber folded into a bent ribbon in which four structural domains can be identified (Lönnroth et al., 1992). Domain 1 is the first one to be synthesized and contains the 5′ end of the pre-mRNA, whereas domain 4 contains the 3′ end. Due to their distinct structure and exceptional dimensions (50 nm in diameter), the BR particles can be identified in situ by morphological criteria using EM.

The BR pre-mRNA has all the features of a typical pre-mRNA and undergoes normal processing. The 5′ end is capped and the nuclear cap binding complex can be detected in situ on the nascent pre-mRNP early after transcription initiation (Visa et al., 1996a). The BR pre-mRNA contains three short introns located close to the 5′ end that are spliced mostly cotranscriptionally (Baurén and Wieslander, 1994). A fourth intron near the 3′ end is removed at the gene locus, but after 3′ end cleavage, in ~80% of the BR pre-mRNA molecules (Baurén et al., 1998). Kinetic experiments in vivo have shown that BR RNA is efficiently exported to the cytoplasm and is highly stable, with an average half-life of ~20 h, as expected for a gene that is actively expressed (Edström et al., 1978, and references therein).

In this study, we have investigated whether the BR particles are bound to any structure that could impair free diffusion through the nucleoplasm. Our results reveal that 31% of the nucleoplasmic BR particles are in contact with thin fibers that in some cases merge into larger nucleoplasmic structures. We have also identified Ct-hrp65 (designated hrp65 for simplicity) as one of the protein components of these thin fibers, which provides a starting point for determining the biological significance of the binding interactions reported here (available from GenBank/EMBL/DDBJ under accession number AJ243013).

Materials and Methods

Animal and Cell Culture

C. tentans and *C. tentans* tissue culture cells were cultivated as described previously (Lezzi et al., 1981; Wyss, 1982).

Antibodies

The mAb 1B7 is an IgM generated by immunization of Balb/c mice with ssDNA-binding proteins from *C. tentans* (Wurtz et al., 1996). The mAb 4E9 is an IgG1 specific for Ct-hrp65 obtained after immunization of mice with pre-mRNPs from *C. tentans* as described by Sun et al. (1998). 2D-Western blot assays showed that the antigen recognized by mAb 4E9 was the Ct-hrp65 protein previously identified by Wurtz et al. (1996). The mAbs 1D3 against hrp23 and 4F9 against hrp36 have been characterized elsewhere (Wurtz et al., 1996; Sun et al., 1998). Serum 282-296 is a polyclonal antiserum against hrp65 raised in rabbits by immunization with a KLH-conjugated synthetic peptide corresponding to amino acids 282–296 of hrp65 (RKSNDYYKARQNGPR). Anti-GST monoclonal antibody is from Sigma. Rabbit anti–mouse immunoglobulins used for immunoprecipitation were purchased from DAKO. Secondary antibodies conjugated with alkaline phosphatase or horseradish peroxidase were also from DAKO. For immuno-EM, secondary antibodies coupled to 6-nm colloidal gold were purchased from Amersham and Jackson ImmunoResearch Laboratories.

Electron Tomography

Salivary glands from *C. tentans* fourth instar larvae were fixed with 2.5% glutaraldehyde in 0.1-M sodium cacodylate-HCl buffer (pH 7.2) containing 0.05-M sucrose. The fixed glands were washed in 0.1-M sodium cacodylate-HCl buffer (pH 7.2), cryoprotected with 2.3-M sucrose in the same buffer, frozen by immersion in liquid nitrogen and stored in liquid nitrogen until further processing. Carbon-coated copper grids (75 × 300 mesh) were glow discharged, incubated with 10-nm colloidal gold solution (AuroProbe EM GAM IgG G10; Amersham) diluted 1/3, rinsed with distilled water, and air dried. Cryosectioning was performed at approximately −105°C. The sections were picked up with a drop of 2.3-M sucrose in sodium cacodylate buffer (pH 7.2) and mounted on the grids. The grids were stained with 2% aqueous uranyl acetate for 5 min, infiltrated in a solution of 4% polyvinyl alcohol (9–10 kD; Aldrich) containing 0.3% uranyl acetate for at least 3–4 min, and picked up with a loop. The excess of liquid was blotted onto a filter paper and the grids were air dried. In control experiments, 20-nm colloidal gold particles were applied on the dry PVA-embedded sections. The grids were rinsed briefly and allowed to air dry as above.

The specimens were imaged in a Philips CEM 200 FEG transmission electron microscope equipped with a cooled 1,024 × 1,024 pixel CCD chip with a pixel size of 24 μm. Automated low-dose tilt series consisting of 61 images (from −60 to +60° every 2°) at 24 610× magnification were recorded using the TVIPS computer interface (TVIPS GmbH). The total dose applied to the specimen was ~100 e/Å^2. Definition of alignment parameters, including determination of x-, y-, and z-coordinates of the used gold markers, was done with an iterative least squares procedure (giving

an alignment error, or gold marker coordinates prediction error, of ~0.6 pixels) and 3D reconstructions were performed according to the filtered back-projection principle at 10 nm resolution as previously described (Skoglund et al., 1986, 1998). The reconstructions were submitted to 10 cycles of refinement against the tilt series data using the Constrained Maximum Entropy Tomography procedure (COMET) (Skoglund et al., 1996). In brief, the COMET refinement generated the most featureless 3D density which projections still fit the observed projections within their variances. The refined reconstructions (~3 nm resolution) were low-pass filtered to 4 nm. The surface rendered images shown in see Fig. 2 d were generated using XTV (Skoglund et al., 1998).

Immuno-EM on Cryosections of Salivary Glands

Immuno-EM was performed as described by Visa et al. (1996b). Dilutions of primary antibodies were 1–10 μg/ml for mAbs, and 1:300 for rabbit preimmune and immune sera. Secondary antibodies were diluted according to manufacturer's recommendations. The specimens were examined and photographed in a Philips CM120 electron microscope at 80 kV under standard high-dose conditions.

Immunostaining of Chromosome Squashes

Salivary glands were fixed in ethanol/acetic acid 3:1 for 5 min and squashed in a drop of 45% acetic acid. The slides were frozen on dry ice, the coverslips pried off, and the preparations were further fixed with 3.7% formaldehyde in PBS for 15 min. The slides were then washed in PBS, dehydrated and stored in absolute ethanol at −20°C. Before immunostaining, the slides were rehydrated, washed with PBSG (PBS containing 0.1-M glycine) for 10 min, and blocked with a solution of 5% nonfat powder milk in PBSG. Incubations with primary antibodies (0.1–1 μg/ml for mAbs, or 1:1,000 for sera) and alkaline-phosphatase secondary antibody were for 1 h and 40 min, respectively. The labeling was visualized using NBT/BCIP.

Preparation of Protein Extracts

Protein extracts for Western blot analyses were prepared from nuclear and cytoplasmic fractions of *C. tentans* tissue culture cells. In brief, the cells were washed in PBS, collected in a glass tissue grinder, homogenized in PBS containing 0.2% NP-40 and 0.1 mM PMSF, and centrifuged at 2,000 *g* for 10 min at 4°C. The supernatant was the cytoplasmic extract used for Western blotting. The pellet containing the nuclei was resuspended in PBS and sonicated for 60 s.

Immunoprecipitation of Pre-mRNP Complexes

Pre-mRNP complexes were immunoprecipitated from nuclear extracts of *C. tentans* tissue culture cells as described by Sun et al. (1998) using either mAb 1D3 (against hrp23) or mAb 4E9 (against hrp65). Control experiments were carried out replacing by PBS either the primary antibody (to detect non specific binding to the protein A–Sepharose) or the nuclear extract (to identify the immunoglobulin chains in the eluted fraction).

Ion-Exchange Chromatography

C. tentans tissue culture cells were resuspended in PBS containing 0.2% NP-40 and 0.5 mM PMSF, homogenized in a glass tissue grinder and centrifuged at 2,000 *g* for 10 min at 4°C. The pellet was washed with PBS containing 0.5 mM PMSF, resuspended in buffer I (Tris-HCl pH 7.5, 25 mM NaCl, 0.1% NP-40, 1 mM EDTA, and 0.5 mM PMSF), and sonicated in ice. The extract was finally centrifuged for 30 min at 7,000 *g* and the supernatant applied to a 2-ml Q-Sepharose Fast Flow (Amersham Pharmacia Biotech) column equilibrated with buffer I. The column was washed with 3 column-volumes of buffer I and the sample was eluted with a linear NaCl gradient (from 25 to 600 mM). Fractions of 1 ml were collected. The proteins in the fractions were precipitated with trichloroacetic acid, washed with acetone, and analyzed by SDS-PAGE and Western blotting.

Protein Electrophoresis and Western Blotting

SDS-PAGE was performed according to standard procedures using 10% polyacrylamide gels in the Mini-Protean II system (Bio-Rad). 2D-gel electrophoresis was carried out in NEPHGE gels using ampholines in the pH 3–10 range. The second dimension was a conventional SDS-PAGE in 10% polyacrylamide minigels. The polyacrylamide gels were stained with either Coomassie or silver. For Western blot, the proteins were transferred onto PVDF membranes (Millipore) in Tris-glycine buffer supplemented with 0.02% SDS and 4-M urea using a semi-dry cell (Bio-Rad). The membranes were blocked with 10% dry milk in PBS before incubation with primary antibody. All antibodies were diluted in PBS containing 1% dry milk and 0.05% Tween-20. The secondary antibodies were conjugated to alkaline phosphatase and developed with NBT/BCIP according to standard procedures. In some cases, the detection was based on ECL chemiluminiscence (Amersham Pharmacia Biotech) using secondary antibodies coupled to horseradish peroxidase.

Protein Microsequencing

The Coomassie stained band containing p65 was excised from the polyacrylamide gel and proteolytic internal peptides were isolated by in-gel digestion as described (Hellman, 1997). In brief, the gel piece was washed and dried, and the protease was forced into the gel matrix during reswelling. After incubation, peptides were extracted and isolated by reversed phase micro-bore liquid chromatography. Selected peptides were subjected to automated Edman degradation in a PE-ABI Procise 494A amino acid sequencer, following the manufacturer's instructions.

Molecular Cloning of hrp65

Poly(A)$^+$ RNA was purified from *C. tentans* tissue culture cells with Oligotex mRNA kit (Qiagen) and reverse-transcribed using an oligo-dT primer. The cDNA was used as a template in a PCR reaction with degenerate oligonucleotides deduced from peptides NFAFLK and TTGEGIVEFAR. This resulted in a product of 260 bp, which was directly cloned into pCRII (Invitrogen) and sequenced. The cloned insert was labeled by PCR with digoxigenin-dUTP (Boehringer Mannheim) and used as a probe to screen a λ-ZAP cDNA library from the salivary glands of *C. tentans* as previously described (Visa et al., 1996b). Four clones were isolated, purified and their inserts were directly amplified by PCR using λ-ZAP SK and T7 primers. The PCR products were purified and directly sequenced using walking primers and ABI PRISM dye terminator kit (Perkin Elmer). The longest clone, λ-hrp65-1, was sequenced at least three times. Sequence analysis was performed with the University of Wisconsin Genetics computer Group Sequence Analysis Programs and EGCG extensions to the Wisconsin Package Sequence Analysis Programs.

Expression of hrp65 in Bacteria

The λ-hrp65-1 clone was used as a template in a PCR reaction to amplify the complete hrp65 open reading frame, using Pfu polymerase (Stratagene) and oligonucleotides designed to introduce a BamHI and a SalI restriction site at the 5′ and 3′ end of the amplified product, respectively. Upon restriction enzyme digestion, the amplified product was cloned into pGEX-4-T1 plasmid (Amersham Pharmacia Biotech) and sequenced to verify correct coding sequence. pGEX-4-T1 and pGEX-4-T1-hrp65-1 were transformed into Bal21 bacterial strain and expression of GST and GST-hrp65 proteins was induced with 1 mM IPTG for 2 h. Purification of recombinant proteins was carried out with glutathione–Sepharose beads (Amersham Pharmacia Biotech), as described by the manufacturer.

Results

In the salivary gland cells of *C. tentans*, the expression of the BR genes can be monitored using electron microscopy and the assembly and transport of BR particles can be directly analyzed in situ (Fig. 1 a). EM observations suggested that BR particles in transit from the gene to the NPC could be associated with thin fibers that extended into the surrounding nucleoplasm (Fig. 1 b). Moreover, a monoclonal antibody (mAb 1B7) was found that labeled the nucleoplasmic fibers associated with BR pre-mRNPs (Fig. 1 c). Such fibers were best preserved in cryo-sections of glands fixed in isotonic conditions (for details see Materials and Methods), although they were also visible in thin sections of plastic-embedded specimens prepared according to classical EM procedures (e.g., Fig. 6 in Skoglund et al., 1983). Single EM images cannot resolve overlapping struc-

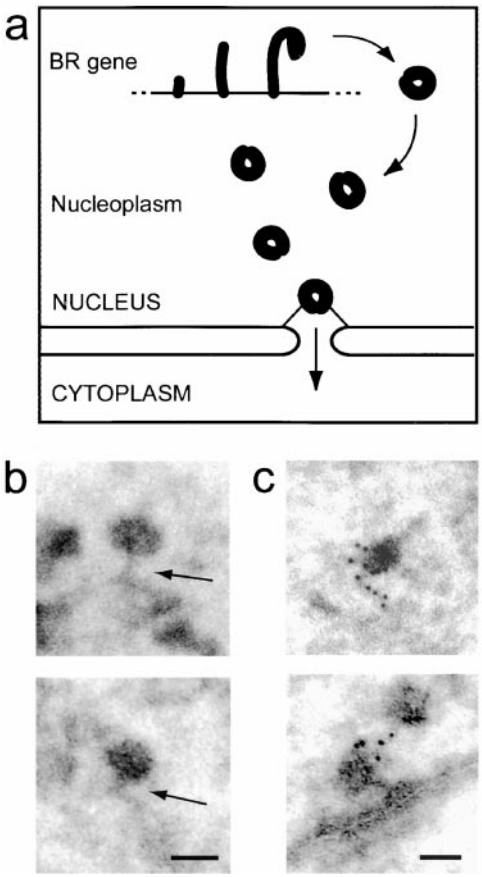

Figure 1. Fibers associated with BR particles in the nucleoplasm of the salivary gland cells. (a) Schematic representation of BR pre-mRNP particles showing successive stages of assembly at the BR gene, transport though the nucleoplasm, and docking at the NPC. (b) Two examples of nucleoplasmic BR particles in a thin cryosection of a salivary gland stained with uranyl acetate and observed in the EM. The BR particles appear as dense granules with a diameter of ~50 nm. The arrows point at fibers that seem to contact the BR particle and extend into the surrounding nucleoplasm. (c) Two examples of fibers immunolabeled with mAb 1B7 and gold-conjugated secondary antibody. The top panel shows a BR particle located in the nucleoplasm, far from both the BR gene and the nuclear envelope. The BR particle shown in the bottom panel is docked at the NPC. Bars, 50 nm.

tures in the electron beam direction, and therefore these initial observations could not rule out the possibility that fibers in the nucleoplasm could occasionally overlap with the BR pre-mRNPs as a consequence of the projection in the EM image, without being really in contact. To circumvent this limitation and obtain reliable 3D information about possible interactions between the pre-mRNPs and other nuclear structures, we analyzed the nucleoplasmic BR particles using ET.

Tomographic Analysis of Nucleoplasmic BR Particles

The tomographic analysis of nucleoplasmic BR particles was carried out on thin cryosections of glutaraldehyde-fixed salivary glands, mildly stained with uranyl acetate and embedded in PVA. The choice of cryosections instead of epoxy-embedded specimens was to avoid harsh dehydration and polymerization treatments that could have detrimental effects on the structure of nuclear fibers, and to avoid protein precipitation effects from the hydrophobic chemicals used in epoxy embedding. We used low-dose EM to minimize damages induced by the electron beam and avoid shrinkage of the specimen. The initial 3D reconstructions were refined by COMET (Skoglund et al., 1996) to remove the high noise level present in the low-dose data. Control experiments were carried out to check that the cryosections would not shrink during the data collection. For this purpose, control grids were prepared with gold markers at both sides of the cryosections, and full tilt series were recorded. The position of each gold marker in the beam direction (Z value) was calculated and expressed as distance from the marker to the central plane of the section. Shrinkage during data collection would cause a decrease in the Z value throughout the tilt series. Fig. 2 a presents a comparison of the Z values calculated for the first half (tilts 1–31) and for the second half (tilts 31–61) of the tilt series. To detect any significant shrinkage, the coordinates of the gold markers in the first half of the tilt series were refined using fixed Z values corresponding to the second half, and vice versa. Swapping over the Z values did not have any significant effect on the refined coordinates. The errors in the predictions of the gold marker positions in the aligned tilt series, 0.76 and 0.71 nm, respectively, were smaller than the pixel size, which indicated no detectable shrinkage above the error of our experiment. We concluded that the cryosections were suitable for ET, at least in the conditions of this study.

The morphology of a typical salivary gland cell in a thin cryosection is shown in Fig. 2 b. The images for tomographic reconstructions were recorded from nucleoplasm regions randomly selected at low magnification. We used 11 independent data sets, and all putative BR particles in each set were selected and reconstructed. Fig. 2 c shows the central tilt (0°) from a data set and illustrates the area selected for the reconstruction of one BR particle. After reconstruction and COMET refinement, the resolution achieved was in the 3-nm range. To facilitate the interpretation of the results in the scope of this study, we low-pass filtered the reconstructed densities to 4 nm. From 106 reconstructions, 52 could be unambiguously identified as BR particles by structural criteria and were further analyzed; the other 54 were discarded. The 52 reconstructed BR particles were classified in three groups (Table I). The first group contained particles that were apparently not in contact with any other structure (Fig. 2 d, I). The second class contained BR particles that were associated with large complexes (Fig. 2 d, II). This group of complex particles was rather heterogeneous: all the reconstructions in this group could be identified as BR particles but the attached structures were of different types. It was impossible to further interpret these complex BR particles due to the little knowledge available about the structure of macromolecular complexes involved in pre-mRNA processing. The third group included BR particles associated with thin fibers (Fig. 2 d, III, IV, and V). Most of the BR particles in this third class presented only one fiber. Only 2 out of 16 BR particles were found with two fibers (not shown). All the fibers had uneven thickness in the 5–7-nm range and were slightly convoluted. In 7 out of 16 cases, the fibers

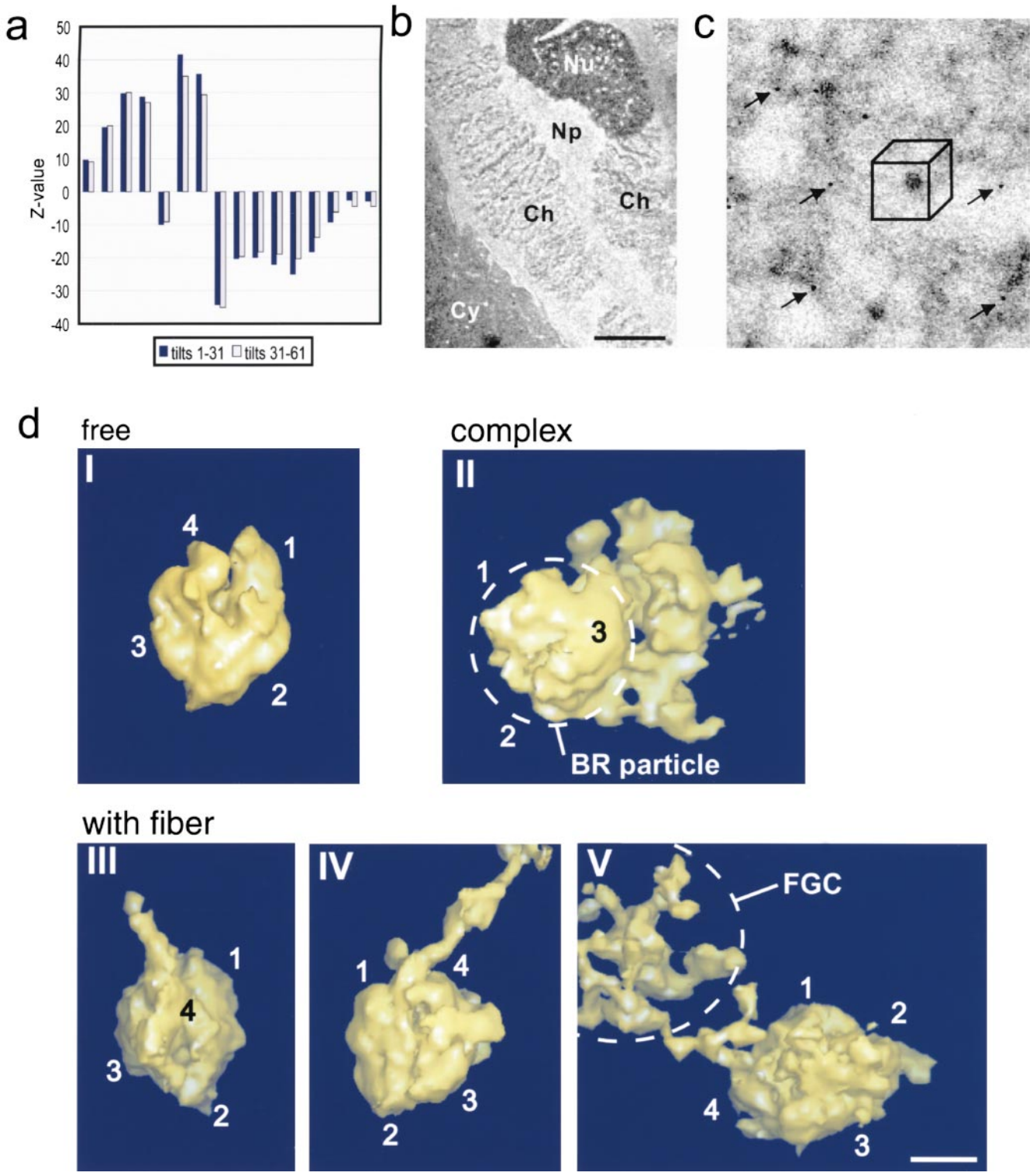

Figure 2. Electron tomographic analysis of nucleoplasmic BR particles. (a) Control experiment to detect possible shrinkage of the specimen during data collection (see text for details). The graph shows the z-values (in pixels) of 16 gold markers in the first (tilts 1-31) and second (tilt 31-61) halves of a tilt series. The 16 gold markers are represented along the x-axis of the graph. Note that a decrease in z-value can be observed for some gold markers, whereas others show increased z-values in tilts 31-61. Therefore, no consistent shrinkage was detected during the data collection. (b) Section through a salivary gland cell as seen in the EM at low magnification. The cytoplasm (Cy) and the nucleus can be easily recognized. The data sets for tomographic reconstructions were recorded from nucleoplasm areas (Np) avoiding nucleolus (Nu) and chromosomes (Ch). (c) Part of the central tilt of one of the data sets used for ET. The cube represents the volume selected for the reconstruction of one putative BR particle. The BR particle appears as a dense granule in the center of the cube. The arrows point at some of the gold markers used in the alignment of the 61 images that constitute one full data set. (d) Analysis of reconstructed BR particles. The numbers on the images (1–4) refer to the domains of the BR particles. All the reconstructions were refined and low-pass filtered to 4 nm. Surrounding densities not directly in contact with the BR particle were cut off to simplify the analysis of the results. I shows an example of an apparently free BR particle, not in contact with any other structure. The BR particle in II is associated with a large complex. BR particles in III, IV, and V are in contact with fibers that extend into the nucleoplasm. The fiber in V is continuous with a fibrogranular cluster (FGC) located in the upper left corner of the image. Bars: (b) 5 μm; (c) the side of the cube is 150 pix, 1 pix = 0.975 nm; (d) 20 nm.

Table I. Classification of Nucleoplasmic BR RNPs Based on Tomographic Reconstructions from 11 Independent Data Sets

Data set	Number of reconstructed BR particles	Number of BR particles in each class		
		Free	Complex	With fiber
1	8	2	4	2
2	2	1	0	1
3	7	2	2	3
4	6	1	4	1
5	2	0	0	2
6	7	2	3	2
7	3	1	2	0
8	2	0	2	0
9	7	1	2	4
10	5	2	3	0
11	3	1	1	1
Total:	52	13	23	16
% in each class:		25	44	31

The criteria used for classification are described in the text.

were short (50 nm or less) and ended inside the volume reconstructed (Fig. 2 d, III). In the rest of the BR particles analyzed, 9/16, the fibers were longer although in most cases could not be traced because they were cut at the edge of the section or reconstruction (Fig. 2 d, IV). In three cases the fibers could be unambiguously traced over longer distances (Fig. 2 d, V) and found to merge into a complex meshwork of interconnected fibers and granules of unknown composition and function that we refer to as fibrogranular cluster (FGC). The FGCs were apparent neither in conventional transmission EM images nor in the single tilts used for tomographic reconstructions. However, after 3D reconstruction and COMET refinement the FGCs appeared as distinct structures in the interchromatin space.

The 11 nucleoplasm regions used for data collection were randomly selected and all data sets gave similar frequencies of BR particles in the three classes (Table I). We did not find any indication for regional differences inside the nucleus, e.g., in relation with distance to the gene or to the nuclear envelope.

We also determined what domain(s) of the BR particle were in contact with the fiber. Using as a reference previously published models of reconstructed BR particles (Lönnroth et al., 1992), we could determine the location of the RNP domains in our reconstructions and establish the position of the contact points. In most cases, at least 12 out of 16, the fibers were bound to the BR particle in the region of contact between domains 1 (containing the 5′ end of the pre-mRNA) and 4 (containing the 3′ end). Only occasionally, 2 out of 16 cases, the BR particles were found with fibers extending from domain 2 (not shown).

In summary, the ET experiments revealed the existence of different populations of nucleoplasmic BR particles. A large fraction of BR particles did not show any morphological sign of attachment to nondiffusible structures at the resolution of the present study. We conclude that the structure of this group, including the class of free particles, the particles with short fibers, and some of the complex BR particles, is compatible with the diffusion models (reviewed by Daneholt, 1999). On the other hand, we also identified a population of BR particles bound to large filamentous structures in the nucleoplasm.

Identification of hrp65 as a Putative Component of the Nucleoplasmic Fibers

The mAb 1B7 labeled the nucleoplasmic fibers by immuno-EM (Fig. 1 c) as well as other cell structures in both nucleus and cytoplasm (data not shown). Western blot assays revealed that mAb 1B7 recognizes three major polypeptides of ~35, 65, and 95 kD in the nuclei of *C. tentans* cells, as well as a 180-kD polypeptide in the cytoplasm (Fig. 3 a).

Wurtz et al. (1996) had identified in *C. tentans* a basic protein of 65 kD, designated Ct-hrp65 (or hrp65 for simplicity), that coimmunoprecipitated with hrp36 and hrp45 and was recognized by mAb 4E9. Immunoprecipitation assays followed by two-dimensional Western blot analysis indicated that the 65-kD protein recognized by mAb 1B7 was the hrp65 protein reported by Wurtz et al. (1996). As shown in Fig. 3 b, the hrp65 protein isolated from a nuclear extract by immunoprecipitation was recognized by mAb 1B7. The two-dimensional gel analysis also indicated that hrp65 was not a single polypeptide but a family of immunologically related isoforms with slight variations in size and pI.

The results reported above suggested that hrp65 was a good candidate to be a component of the pre-mRNP-associated fibers. With the aim of confirming this possibility, we performed immuno-EM experiments with the mAb 4E9 specific for hrp65. However, this antibody was found to be sensitive to the glutaraldehyde fixation used for im-

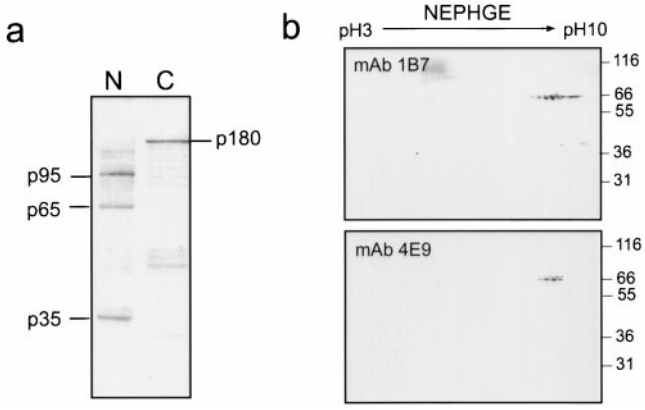

Figure 3. The 65-kD protein recognized by mAb 1B7 is hrp65. (a) Specificity of mAb 1B7 in Western blot of *C. tentans* proteins. Proteins of nuclear (N) and cytoplasmic (C) fractions were separated by SDS-PAGE, blotted to transfer membranes and probed with mAb 1B7. (b) Reactivity of mAb 1B7 against the hrp65 protein immunoprecipitated by mAb 4E9. Pre-mRNP complexes were immunoprecipitated from *C. tentans* nuclear extracts with mAb 4E9 specific for hrp65. The immunoprecipitated proteins were analyzed by 2D-Western blot using mAb 1B7 (top). The bottom panel shows the specificity of mAb 4E9 in 2D-blots of *C. tentans* nuclear proteins. Note that both mAbs recognize the same group of spots in the basic region of the gel. Approximate antibody concentrations: 1 μg/ml for 1B7, 0.2 μg/ml for 4E9, and 1 μg/ml for the alkaline phosphatase-conjugated secondary antibody. The mobility of molecular mass standards is indicated in kD.

muno-EM and failed to give any labeling in this type of assays. The localization of hrp65 in pre-mRNP–associated fibers was confirmed later on using an anti-hrp65 antibody raised against a synthetic peptide (see below).

Cloning of hrp65 cDNA

The hrp65 protein was partially purified by ion-exchange chromatography from a nuclear extract made from *C. tentans* tissue culture cells. Fractions containing hrp65 were identified by Western blot using mAb 1B7 and pooled together. Hrp65 was resolved by SDS-PAGE, excised from the gel and subjected to proteolytic digestion. Six peptides were isolated and sequenced with the following results: MQLEEEKLEAQME, ELFS, IRDEQ?Y?MR, AVIIVDDR, TTGEGIVEFAR and NFAFLK. Degenerate oligonucleotides corresponding to these amino acid sequences were used in different combinations to prime *C. tentans* cDNA in a PCR reaction (see Materials and Methods). A 260-bp PCR product obtained with oligonucleotides corresponding to peptides TTGEGIVEFAR and NFAFLK was labeled and used to screen a *C. tentans* salivary gland cDNA library. Four positive clones were identified. The longest one, λ-hrp65-1, was found to have a 2,200-bp insert that included a 5′UTR (91 nt), an open reading frame (1,605 nt) capable of encoding a protein of 535 amino acids, a 3′UTR (513 nt) and a poly(A)stretch. There were five in-frame stop codons upstream of the first initiation codon, which perfectly matched the consensus translation initiation site for eukaryotic RNAs (Kozak, 1986).

The protein encoded by clone λ-hrp65-1 had a predicted molecular mass of 62 kD and contained several putative phosphorylation and glycosylation sites. The estimated isoelectric point of the protein was 9.64, in agreement with the basic behavior of hrp65 in NEPHGE (Fig. 3 b; Wurtz et al., 1996).

To obtain specific antibodies against hrp65 that could be used in immuno-EM, antibodies were raised in rabbits against a synthetic peptide encompassing amino acid residues 282–296 from hrp65 (serum 282–296). As shown in Fig. 4 a, the serum 282–296 solely recognized a protein of 65 kD that comigrated with the protein labeled by mAb 4E9, whereas no band was observed with the pre-immune serum. To further demonstrate that the protein encoded by the λ-hrp65-1 clone was indeed the hrp65 protein recognized by mAbs 1B7 and 4E9, the open reading frame of λ-hrp65-1 was linked to the GST ORF and expressed in *E. coli*. The recombinant GST-hrp65 protein had an apparent molecular mass of ~88 kD. Considering that the GST moiety was 26 kD, the resulting size for hrp65 was 62 kD, in agreement with its predicted molecular mass. Western blot assays (Fig. 4 b) showed that both 1B7 and 4E9 recognized the bacterially expressed GST-hrp65 protein, but not the GST protein alone, indicating that they specifically immunoreact with hrp65. As expected, the serum 282–296 also detected the recombinant fusion protein.

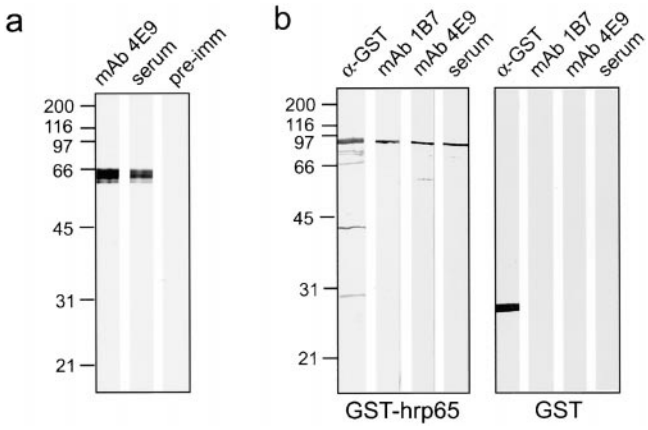

Figure 4. Immunoreactivity of *C. tentans* hrp65 and bacterially expressed hrp65-GST fusion protein. (a) Western blot analysis of hrp65 in extracts from *C. tentans* tissue culture cells. Nuclear proteins were extracted, separated by SDS-PAGE and blotted to transfer membranes. The membranes were cut into strips and incubated with either monoclonal antibody 4E9 or serum 282-296. The same pattern of labeling is observed with both antibodies. The pre-immune serum was negative. (b) Expression of the protein encoded in cDNA clone λ-hrp65-1 in bacteria. The coding region of λ-hrp65-1 was fused in-frame with the GST protein and the hrp65-GST fusion protein was expressed in *E. coli*. The GST protein alone was expressed in parallel. The recombinant proteins were purified and analyzed by Western blotting with an anti-GST monoclonal antibody, mAb 1B7, mAb 4E9 and serum 282-296, as indicated above the lanes. Note that the hrp65-GST fusion protein is recognized by all the antibodies, whereas the GST alone is only labeled by the anti-GST antibody. The mobility of molecular mass standards is indicated in kD.

The Sequence of hrp65

The amino acid sequence predicted from the cDNA clone λ-hrp65-1 revealed a central region with two classical RNA-binding domains (RBD1 and RBD2) containing the RNP-1 and RNP-2 consensus sequences (Burd and Dreyfuss, 1994), and two auxiliary domains (Fig. 5 a). The amino-terminal auxiliary domain was rich in asparagine (21%), glycine (13%), lysine (10%), and proline (10%), and did not reveal any significant sequence similarity to any other known protein. The hrp65 carboxy-terminal domain was rich in glycine (23%), asparagine (20%), glutamine (14%), and arginine (10%). Some of these amino acids were organized in two glycine clusters with five interspersed GGN tripeptides.

Searches in the SWISS-PROT database (Bairoch and Boeckmann, 1993) revealed that hrp65 had a strong sequence similarity to RNA-binding proteins. The highest similarity score was obtained with the *Drosophila* NoNa protein (Jones and Rubin, 1990; von Besser et al., 1990). The amino acid identity between the two proteins was 53% and the similarity 64%. The human $p54^{nrb}$ and PSF proteins (Dong et al., 1993; Patton et al. 1993) also proved to be very similar to hrp65, with ~36% identical and 48% similar amino acid residues. Most of this extensive sequence homology resided within a central region of 320 amino acids, the so-called DBHS (*Drosophila* behavior and human splicing) domain (Dong et al., 1993), which is a common feature of NoNa, $p54^{nrb}$, PSF, and hrp65 (Fig. 5 b). The DBHS domain includes the two RBDs plus additional 100 amino acids downstream of unknown function.

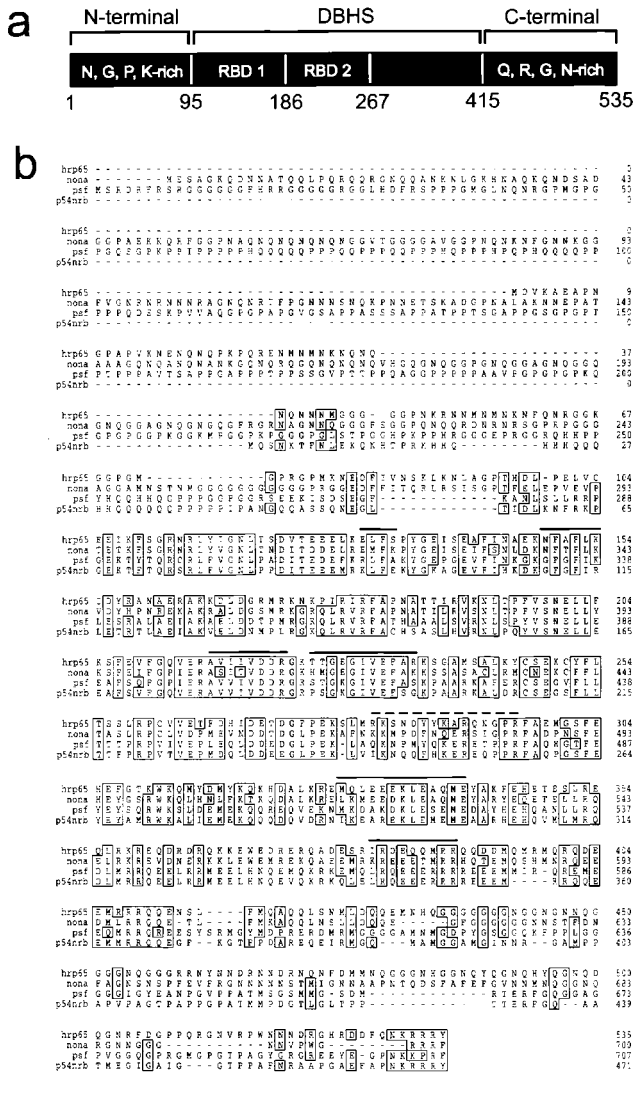

Figure 5. Amino acid sequence of hrp65 and sequence comparison with *Drosophila* NoNa and human PSF and p54^{nrb}. (a) Schematic representation of *C. tentans* hrp65. Protein domains are boxed and amino acid residues in the boundaries between the distinct domains are shown below the diagram. (b) The amino acid sequences of hrp65, *Drosophila* NoNa and human PSF and p54^{nrb} were compared and aligned using the PILEUP and PRETTYPLOT programs. Similar residues in at least 3 of the 4 compared sequences are boxed. Solid lines on the hrp65 sequence indicate the microsequenced peptides, whereas the dashed line shows the peptide used to generate serum 282-296.

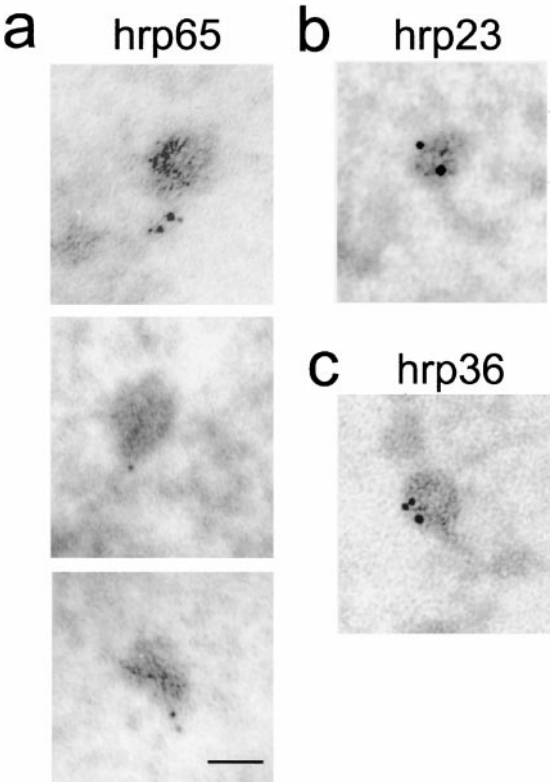

Figure 6. Localization of hrp65 in CFs. (a) Immuno-EM localization of hrp65 on thin cryosections of salivary glands. The sections were incubated with serum 282-296, and with a gold-conjugated secondary antibody. Three examples of fibers associated with BR particles and decorated with gold markers are presented. Note that the labeling is not located on the BR particle itself, but on the proximal segment of the fiber. (b and c) Immuno-EM localization of hrp23 and hrp36, respectively, on thin cryosections of salivary glands. Note that hrp23 and hrp36 are located in the BR particle itself but not on the CF. Bar, 50 nm.

Localization of hrp65

The serum 282-296 was used to confirm the location of the hrp65 protein in the nucleoplasmic fibers. We performed immuno-EM experiments using cryo-sections of salivary gland cells from *C. tentans*. The sections were first incubated with the serum 282-296 and subsequently with a gold-conjugated anti-rabbit antibody. As expected, the gold markers were mainly located in the nucleus and the nucleoplasmic fibers were often decorated by gold markers (Fig. 6 a), which confirmed that hrp65 was indeed a component of these novel structures. Moreover, the immuno-EM analysis revealed that hrp65 was not present along the whole length of the fiber but exclusively in the segment close to the BR particle.

The possible presence of hrp65 in the BR particle itself, and not only in the fiber, could not be totally ruled out. A fraction of hrp65 could be buried in the pre-mRNP and inaccessible to the 282-296 peptide antibody, or posttranslationally modified in a way that could impair antibody recognition. However, we favor the interpretation that hrp65 is not present in the BR particle because labeling with mAb 1B7 was also seen preferentially on the fibers (Fig. 1 c).

The location of hrp65 was compared with that of other hrp proteins known to be present in the BR particles. Antibodies against hrp23 (Fig. 6 b) and hrp36 (Fig. 6 c) labeled the BR particle, in agreement with previous reports (Visa et al., 1996b; Sun et al., 1998), but failed to label the fiber. From these observations we conclude that the fibers have a specific protein composition that is different from that of the BR particles: the fibers are characterized by presence of hrp65 and absence of other hrps such as hrp23 and hrp36.

Comparing the immuno-EM results obtained with mAb 1B7 (Fig. 1 c) and serum 282-296 (Fig. 6 a), it is clear that

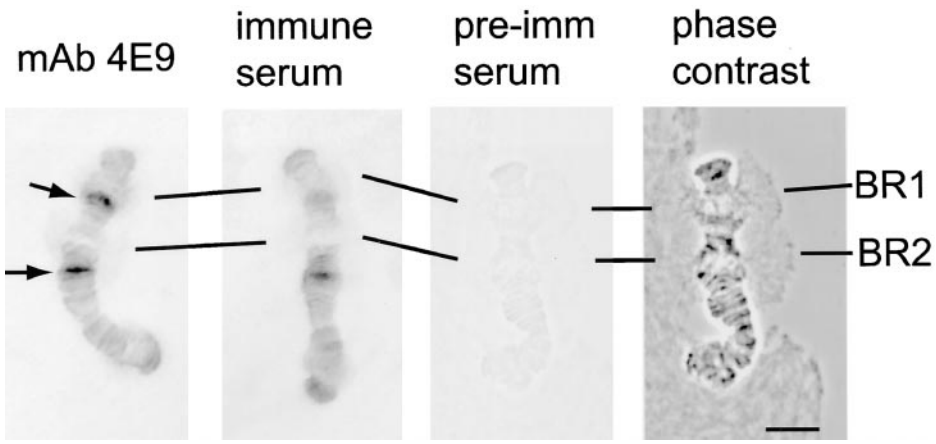

Figure 7. Localization of hrp65 in polytene chromosomes of *C. tentans*. Polytene chromosome preparations were incubated with either mAb 4E9 or serum 282-296, and the immunoreactive sites were detected with alkaline phosphatase-conjugated secondary antibodies. The figure shows the labeling of chromosome IV, where the BR genes are located. The large puffs BR1 and BR2, indicated in the phase contrast photograph, are not labeled by any of the two antibodies. A few other loci in chromosome IV are labeled with both mAb 4E9 and serum 282-296 (arrows). Bar, 10 μm.

the former resulted in a stronger signal. This difference might be explained by signal amplification due to the fact that 1B7 is an IgM. On the other hand, taking into account the complex specificity of mAb 1B7 (e.g., Fig. 3 a), we cannot exclude the possibility that mAb 1B7 could recognize additional proteins also located in the nucleoplasmic fibers.

We also investigated whether the hrp65 protein was bound to the BR particles cotranscriptionally. To answer this question, preparations of polytene chromosome were immunostained with anti-hrp65 antibodies (Fig. 7). The results revealed a number of immunoreactive loci but the large puffs BR1 and BR2 on chromosome IV, where the BR genes are transcribed, were clearly negative. Identical results were obtained with mAb 4E9 and serum 282-296. The pre-immune serum was negative. These results demonstrated that hrp65 does not bind to BR pre-mRNPs on the chromosome. We conclude that the interaction between hrp65 and the BR particles occurs posttranscriptionally.

Discussion

Using ET we have studied the 3D structure of BR particles in transit from the gene to the NPC. Our data revealed that nucleoplasmic BR particles constitute a very heterogeneous population. There is a fraction of apparently free BR particles (~25%), a population of BR particles associated with large complexes (44%) and a third population bound to fibers (31%) that in some cases merge into an intricate fibrogranular meshwork. According to Edström et al. (1978), 80–100% of the BR RNA is exported to the cytoplasm, which implies that all three types of BR particles do eventually leave the nucleus and can therefore be regarded as different intermediates in the processing/export pathway.

The population of BR particles associated with fibers reveals the existence of two novel structures: a thin connecting fiber (CF) that is in contact with the BR particle, and a fibrogranular cluster (FGC) to which the CF becomes occasionally attached. CFs and FGCs are structurally continuous but the observation that hrp65 is present exclusively in CFs supports the interpretation that CFs and FGCs are different structures.

CFs can be observed under different preparative conditions (i.e., hydrophobic plastic embedding and hydrophilic cryosections), which argues against the possibility that they could be artifacts. The specificity of the CFs is also supported by the observation that they have a preferential attachment site on the BR particle, and by their specific protein composition. Our present data is based on 3D reconstructions of small nucleoplasmic volumes and therefore we cannot state neither the dimensions of full FGCs nor whether they are interconnected or associated with other nuclear structures. Further research is required to elucidate FGC's structure, composition and function.

Even in the absence of kinetic data, the structural results presented here provide relevant information about binding interactions that impose restrictions on the type of movement of the BR particles. We can infer the following conclusions. First, the structure of the so-called free BR particles is compatible with the proposal that intranuclear transport of pre-mRNPs is based on diffusion phenomena. Second, at least some of the pre-mRNPs in transit from the gene to the nuclear pore interact with specific nuclear structures, i.e., CFs and FGCs. Third, the BR particles attached to FGCs via CFs cannot diffuse freely at rates estimated for single BR particles. We cannot rule out the possible diffusion of a complex containing BR particles, CFs and FGCs. However, the diffusion properties of such a large complex would differ significantly from those of single pre-mRNPs. Fourth, from the existence of apparently free BR particles not in contact with CFs, and considering that hrp65 is absent from the BR transcription sites, we can also conclude that the interaction between CFs and BR particles is a transient, posttranscriptional event.

In summary, our results are compatible with the proposal that a large fraction of pre-mRNPs are free to diffuse in the nucleoplasm (reviewed by Daneholt, 1999) but we also provide direct evidence for physical interactions between the pre-mRNP and other nuclear structures. These observations imply that nucleoplasmic pre-mRNPs are not always freely diffusible and that some of the posttranscriptional events that the pre-mRNP undergoes before reaching the NPC occur in a bound state.

The hrp65 Protein

We have identified hrp65 as one of the protein components of the CFs associated with BR particles. The hrp65 protein had been previously identified by Wurtz et al. (1996) in a 2D-electrophoretic analysis of immunoprecipitated hnRNP proteins. We have now cloned and sequenced a cDNA encoding hrp65 and the primary sequence of this new protein is presented here.

The hrp65 protein has two features in common with hrps present in the BR particles, such as hrp23 (Sun et al., 1998), hrp36 (Visa et al., 1996b), and hrp45 (Alzhanova-Ericsson et al., 1996). First, all these proteins have a modular primary structure containing one or two RBDs. Second, they can all be coimmunoprecipitated from nuclear extracts, which suggested that they are part of the same hnRNP complexes (Wurtz et al., 1996). However, our immuno-EM study suggests that hrp65 is located in the fibers that are connected to the BR particle and not in the BR particle itself. Moreover, hrp23, hrp36, and hrp45 bind to the BR pre-mRNA cotranscriptionally, as expected for hnRNP proteins, whereas we failed to detect binding of hrp65 to the chromosomal BR pre-mRNA, in agreement with observations by Singh, O.P., N. Visa, and B. Daneholt (manuscript in preparation). In conclusion, due to its different localization, hrp65 cannot be classified as a typical hnRNP protein.

Another interesting finding is the presence of a DBHS domain in the hrp65 protein and the high similarity to other proteins such as $p54^{nrb}$, PSF, and NoNa/BJ6. The PSF protein is a human splicing factor associated with the polypyrimidine tract-binding protein that can also bind directly to the polypyrimidine tract of mammalian introns (Patton et al., 1993). The human $p54^{nrb}$ protein can bind to both mRNA and DNA, and it can act as a transcription activator (Basu et al., 1997). Mutations in the gene that encodes NoNa/BJ6 have pleiotropic effects in the central nervous system of *Drosophila* (Rendahl et al., 1992, and references therein) and it has been proposed that the NoNa/BJ6 function is related to splicing regulation (Dong et al., 1993). In summary, these proteins appear to play different roles in gene expression, and the mere presence of a DBHS domain in hrp65 does not provide conclusive information about its function. The auxiliary domains are likely to be essential to define the functional properties of each protein, and it is interesting to note that the amino-terminal domain of hrp65 is not similar to any protein in the databases.

Although hrp65 is not present in the BR puffs, we could detect hrp65 in a number of other loci in the polytene chromosomes (Fig. 7). This observation suggests that the formation of CFs on pre-mRNPs from other genes might occur cotranscriptionally. Alternatively, and considering the role of $p54^{nrb}$ in transcription (Basu et al., 1997), the chromosomal fraction of hrp65 could be engaged instead in transcription regulation.

CFs Mediate Binding of Pre-mRNPs to Other Nucleoplasmic Structures

CFs associated with nucleoplasmic BR particles can be of variable length, and only some of them make contact with FGCs. The most simple interpretation of these observations is that CFs assemble on the pre-mRNP particle and subsequently interact with pre-existing FGCs in the nucleoplasm. We propose that once the assembly of a CF has been initiated, an elongation process takes place by binding of additional protein molecules to the growing CF. Considering that the longest CFs are 50–100 nm long, and that an average globular protein has a diameter of ~3 nm, the longest CFs could contain ~100 protein molecules. On the other hand, from the immuno-EM experiments we infer that hrp65 cannot be the only component of the CFs because antibodies against hrp65 label exclusively the segment of the CFs close to the BR particles. Thus, additional protein/s must be present in the CFs, at least in the distal segment.

Many questions arise in relation to the molecular mechanisms that result in the formation of CFs. We would like to understand what is the signal or feature of the BR particle that triggers the assembly of the CF, whether this feature is RNA or protein, and whether the hrp65 protein is involved in this initial recognition step. The hrp65 protein has two RNA-binding domains and PSF is able to bind to polypyrimidine-rich sequences (Patton et al., 1993). These two facts suggest that hrp65 can bind to the pre-mRNA directly. However, binding of hrp65 to the pre-mRNA would result in the presence of hrp65 at the sites of transcription and in our experiments hrp65 was not detectable at the chromosomal level. Therefore, we favor the hypothesis that hrp65 does not bind to the BR pre-mRNA directly and that there is a previous step, maybe binding of another protein to the BR particle, before hrp65 can be incorporated into the new CF.

The BR pre-mRNP particle is a bent ribbon in which domains 1 and 4, containing the 5′ and 3′ ends of the pre-mRNA, respectively, are in close proximity (Skoglund et al., 1986). It is remarkable that most of the CFs observed in this study make contact with the BR particle just in the region where domains 1 and 4 come together. This suggests that the assembly of the CF could start by recognition of unique features of the 5′ or 3′ ends. Alternatively, the CFs might be related to the presence of introns or splicing factors. This possibility would also be compatible with attachment of the CF to domains 1 or 4 because the BR pre-mRNAs contain three introns close to the 5′ end and one intron close to the 3′ end, whereas domains 2 and 3 include exonic sequences exclusively (Wieslander, 1994).

In summary, our results suggest the following series of events leading to the attachment of BR particles to FGCs (Fig. 8). First, the assembly of an CF is initiated on the BR particle. Second, the initial CF is elongated by addition of protein molecules to the growing end. Third, the free end of the CF makes contact with a FGC. Whether the BR particle is subsequently released, or actively transported to the NPC in a nondiffusible state remains to be elucidated.

Structural Complexity of the Nucleoplasm

The results of our ET study provide direct evidence for the high structural complexity of the nucleoplasmic compartment, which appears to contain complex aggregates of interconnected fibers and granules that we refer to as FGCs. Moreover, BR particles interact with these FGCs before being exported to the cytoplasm, which argues in favor of

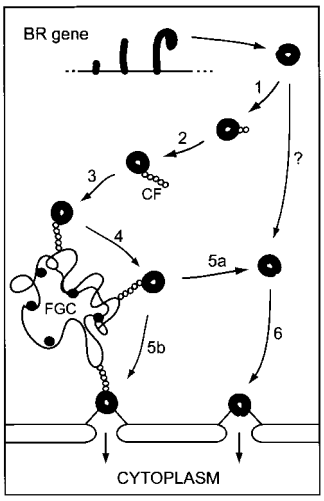

Figure 8. A model for the intranuclear movement of the BR particle. The newly synthesized BR pre-mRNP particle is released into the nucleoplasm and the assembly of a connecting fiber (CF) is initiated upon recognition of a specific feature in the pre-mRNP (1). The hrp65 protein is located in the proximal segment of the CF and is likely to be involved in early assembly steps. The initial CF is elongated by binding of additional protein molecules (2). Eventually the CF attaches the BR particle (3) to a large fibrogranular cluster (FGC) where the BR pre-mRNP is sorted/processed/transported (4). The BR particle is subsequently released into the nucleoplasm (5a) and can reach the NPC by free diffusion (6). Alternatively, the BR particle might be transported to the NPC in a guided manner (5b).

a role for these structures in pre-mRNA metabolism. It is important to notice that neither the CFs nor the FGCs are chromatin fibers: in the polytene nuclei used in our study the DNA is located exclusively in the polytene chromosomes, which leaves the nucleoplasm free of chromatin.

The key molecules involved in pre-mRNA synthesis, processing, and export appear to be highly conserved during evolution, and thus CFs and FGCs are not likely to be exclusive of insect polytene cells. Some nuclear structures have been described that could be related to CFs and FGCs. One of them is the nuclear matrix (reviewed in Pederson, 1998). Although we have not performed any detailed comparison, the nucleoplasmic structures reported in this study do not resemble the filaments of the nuclear matrix. Perhaps the most remarkable difference is that FGCs appear as relatively compact structures that occupy discrete regions of the nucleoplasm, whereas the nuclear matrix preparations reveal a meshwork of fibers that extend throughout the whole interior of the nucleus (e.g., Fey et al., 1986).

The second type of structures that should be considered in this context are the interchromatin granules found in a variety of plant, animal and fungi cells (for review see Puvion and Puvion-Dutilleul, 1996). The interchromatin granule clusters (IGCs) are known to be dynamic structures that serve as storage and/or reassembly sites for splicing factors (Misteli and Spector, 1998). Moreover, IGCs are likely to play additional roles in sorting/transport of pre-mRNAs. Interestingly, several studies have shown that pre-mRNAs accumulate transiently in IGCs during intranuclear transport (e.g., Puvion-Dutilleul et al., 1997; Bridge et al., 1996). These findings suggest that the *Chironomus* FGCs could be the insect counterpart of the mammalian IGCs.

The NPC-attached filaments containing Tpr protein (Cordes et al., 1997) also share some features with the nucleoplasmic fibers reported here. In *Drosophila*, the Tpr protein is not only located at the nuclear periphery but it extends deep inside the nucleus and reaches the periphery of the chromosomes (Zimowska et al., 1997). Moreover, a recent report has shown that two Tpr homologues in yeast, Mlp1p and Mlp2p, are part of intranuclear structures that might be involved in the translocation of macromolecules between the nucleoplasm and the NPC (Strambio-de-Castillia et al., 1999). It will be interesting to investigate whether CFs and FGCs are related to the Tpr filaments.

The most interesting question arising from our conclusions is the functional significance of the CFs in relation to pre-mRNA processing and/or export. The binding interaction that we report must necessarily affect the mobility of the pre-mRNP, but with the present data we cannot conclude whether the interaction will restrict or promote movement. Binding to FGCs via CFs might represent a mechanism for sorting and nuclear retention of unprocessed transcripts; nuclear retention could be mediated by the presence of proteins bearing nuclear retention signals in the pre-mRNP (Nakielny and Dreyfuss, 1996), by the presence of introns in the pre-mRNA (Legrain and Rosbash, 1989), or by incomplete 3′ end processing (Custódio et al., 1999). Alternatively, the CFs might be involved in active, guided transport of pre-mRNPs from the nucleoplasm to the NPC in a late step of intranuclear transport (Strambio-de-Castillia et al., 1999, and references therein). The functional characterization of CFs, and in particular the identification of proteins interacting with hrp65, should help to elucidate the molecular composition of CFs and to understand their role in mRNA biogenesis.

We thank S. Masich for the gift of carbon-coated copper grids, L. Fjelkestam for technical assistance, and L. Wieslander for constructive criticism.

This work has been supported by grants from NFR (dnr B-AA/BU 11617-301/302), Marianne and Marcus Wallenberg Foundation, Jeansson Foundation, Karolinska Institute, and Lars Hiertas Minne Foundation to N. Visa, and grants from TFR (dnr 97-721-230), EU (BIO4-CT97-2364 and BIO4-CT96-0099) and FRN (dnr 960783) to U. Skoglund. F. Miralles is recipient of a long-term postdoctoral fellowship from EMBO. N. Sabri is supported by a scholarship from the Ministry of Culture and Higher Education (Iran).

Submitted: 8 October 1999
Revised: 3 December 1999
Accepted: 8 December 1999

References

Agutter, P.S. 1995. Intracellular structure and nucleocytoplasmic transport. *Int. Rev. Cytol.* 162B:183–224.

Alzhanova-Ericsson, A.T., X. Sun, N. Visa, E. Kiseleva, T. Wurtz, and B. Daneholt. 1996. A protein of the SR family of splicing factors binds extensively to exonic Balbiani ring pre-mRNA and accompanies the RNA from the gene to the nuclear pore. *Genes Dev.* 10:2881–2893.

Bairoch, A., and B. Boeckmann. 1993. The SWISS-PROT protein sequence data bank, recent developments. *Nucleic Acids Res.* 21:3093–3096.

Basu, A., B. Dong, A.R. Krainer, and C.C. Howe. 1997. The intracisternal A–particle proximal enhancer-binding protein activates transcription and is identical to the RNA- and DNA-binding protein p54nrb/NonO. *Mol. Cel. Biol.* 17:677–686.

Baurén, G., and L. Wieslander. 1994. Splicing of Balbiani ring 1 gene pre-mRNA occurs simultaneously with transcription. *Cell.* 76:183–192.

Baurén, G., S. Belikov, and L. Wieslander. 1998. Transcriptional termination in the Balbiani ring 1 gene is closely coupled to 3′-end formation and excision of the 3′-terminal intron. *Genes Dev.* 12:2759–2769.

Bridge, E., K.U. Riedel, B.M. Johansson, and U. Pettersson. 1996. Spliced exons of adenovirus late RNAs colocalize with snRNP in a specific nuclear domain. *J. Cell Biol.* 135:303–314.

Burd, C.G., and G. Dreyfuss. 1994. Conserved structures and diversity of functions of RNA-binding proteins. *Science.* 265:615–621.

Cordes, V.C., S. Reidenbach, H.-R. Rackwitz, and W.W. Franke. 1997. Identifi-

cation of protein p270/Tpr as a constitutive component of the nuclear pore complex-attached intranuclear filaments. *J. Cell Biol.* 136:515–529.

Custódio, N., M. Carmo-Fonseca, F. Geraghty, H.S. Pereira, F. Grosveld, and M. Antoniou. 1999. Inefficient processing impairs release of RNA from the site of transcription. *EMBO (Eur. Mol. Biol. Organ.) J.* 18:2855–2866.

Daneholt, B. 1999. Pre-mRNP particles: from gene to nuclear pore. *Curr. Biol.* 9:412–415.

Dong, B., D.S. Horowitz, R. Kobayashi, and A.R. Krainer. 1993. Purification and cDNA cloning of HeLa cell p54nrb, a nuclear protein with two RNA recognition motifs and extensive homology to human splicing factor PSF and *Drosophila* NONA/BJ6. *Nucleic Acids Res.* 21:4085–4092.

Edström, J.E., E. Ericson, S. Lindgren, U. Lönn, and L. Rydlander. 1978. Fate of Balbiani-ring RNA *in vivo*. *Cold Spring Harbor Symp. Quant. Biol.* 42: 877–884.

Fey, E.G., G. Krochmalnic, and S. Penman. 1986. The nonchromatin substructures of the nucleus: the ribonucleoprotein (RNP)-containing and RNP-depleted matrices analyzed by sequential fractionation and resinless section electron microscopy. *J. Cell Biol.* 102:1654–1665.

Hellman, U. 1997. Isolation of peptides for microsequencing by in-gel proteolytic digestion. *In* Protein Structure Analysis. Preparation, characterization, and microsequencing, R.M. Kamp, T. Choli-Papadopoulou and B. Wittmann-Liebold, editors. Springer-Verlag, Heidelberg. 97–104.

Izaurralde, E., A. Jarmolowski, C. Beisel, I.W. Mattaj, G. Dreyfuss, and U. Fischer. 1997. A role for the M9 transport signal of hnRNP A1 in mRNA nuclear export. *J. Cell Biol.* 137:27–35.

Jones, K.R., and G.M. Rubin. 1990. Molecular analysis of no-on-transient A, a gene required for normal vision in *Drosophila*. *Neuron.* 4:711–723.

Kozak, M. 1986. Point mutations define a sequence flanking the AUG initiator codon that modulates translation by eukaryotic ribosomes. *Cell.* 44:283–292.

Krecic, A.M., and M.S. Swanson. 1999. HnRNP complexes: composition, structure, and function. *Curr. Opin. Cell Biol.* 11:363–371.

Legrain, P., and M. Rosbash. 1989. Some cis- and trans-acting mutants for splicing target pre-mRNA to the cytoplasm. *Cell.* 57:573–583.

Lezzi, M., B. Meyer, and R. Mähr. 1981. Heat shock phenomena in *Chironomus tentans*. I: *In vivo* effects of heat, overheat, and quenching on salivary chromosome puffing. *Chromosoma.* 83:327–339.

Lönnroth, A., K. Alexciev, H. Mehlin, T. Wurtz, U. Skoglund, and B. Daneholt. 1992. Demonstration of a 7-nm RNP fiber as the basic structural element in a premessenger RNP particle. *Exp. Cell. Res.* 199:292–296.

Mattaj, I.W., and L. Englmeier. 1998. Nucleocytoplasmic transport: the soluble phase. *Annu. Rev. Biochem.* 67:265–306.

Michael, W.M., M. Choi., and G. Dreyfuss. 1995. A nuclear export signal in hnRNP A1: a signal-mediated, temperature-dependent nuclear protein export pathway. *Cell.* 83:415–422.

Misteli, T., and D.L. Spector. 1998. The cellular organization of gene expression. *Curr. Opin. Cell Biol.* 10:323–331.

Nakielny, S., and G. Dreyfuss. 1996. The hnRNP C proteins contain a nuclear retention sequence that can override nuclear export signals. *J. Cell Biol.* 134: 1365–1373.

Patton, J.G., E.B. Porro, J. Galceran, P. Tempst, and B. Nadal-Ginard. 1993. Cloning and characterization of PSF, a novel pre-mRNA splicing factor. *Genes Dev.* 7:393–406.

Pederson, T. 1998. Thinking about a nuclear matrix. *J. Mol. Biol.* 277:147–159.

Politz, J.C., E.S. Browne, D.E. Wolf, and T. Pederson. 1998. Intranuclear diffusion and hybridization state of oligonucleotides measured by fluorescence correlation spectroscopy in living cells. *Proc. Natl. Acad. Sci. USA.* 95:6043–6048.

Puvion, E., and F. Puvion-Dutilleul. 1996. Ultrastructure of the nucleus in relation to transcription and splicing: roles of perichromatin fibrils and interchromatin granules. *Exp. Cell Res.* 229:217–225.

Puvion-Dutilleul, F., S. Besse, J.J. Diaz, K. Kindbeiter, M. Vigneron, S.L. Warren, C. Kedinger, J.J. Madjar, and E. Puvion. 1997. Identification of transcription factories in nuclei of HeLa cells transiently expressing the Us11 gene of herpes simplex virus type 1. *Gene Expr.* 6:315–332.

Rendahl, K.G., K.R. Jones, S.J. Kulkarni, S.H. Bagully, and J.C. Hall. 1992. The dissonance mutation at the no-on-transient-A locus of *D. melanogaster*: genetic control of courtship song and visual behaviors by a protein with putative RNA-binding motifs. *J. Neurosci.* 12:390–407.

Singh, O.P., B. Björkroth, S. Masich, L. Wieslander, and B. Daneholt. 1999. The intranuclear movement of Balbiani ring pre-messenger ribonucleoprotein particles. *Exp. Cell. Res.* 251:135–146.

Skoglund, U., K. Andersson, B. Björkroth, M.M. Lamb, and B. Daneholt. 1983. Visualization of the formation and transport of a specific hnRNP particle. *Cell.* 34:847–855.

Skoglund, U., K. Andersson, B. Strandberg, and B. Daneholt. 1986. Three-dimensional structure of a specific pre-messenger RNP particle established by electron microscope tomography. *Nature.* 319:560–564.

Skoglund, U., L.-G. Öfverstedt, R.M. Burnett, and G. Bricogne. 1996. Maximum-entropy three-dimensional reconstruction with deconvolution of the contrast transfer function: a test application with adenovirus. *J. Struct. Biol.* 117:173–188.

Skoglund, U., L.-G. Öfverstedt, and B. Daneholt. 1998. Procedures for three-dimensional reconstruction from thin sections with electron tomography. *In* RNP Particles, Splicing and Autoimmune Diseases. J. Schenkel, editor. Springer Verlag, Berlin, Heidelberg, New York. 72–94.

Strambio-de-Castillia, C., G. Blobel, and M.P. Rout. 1999. Proteins connecting the nuclear pore complex with the nuclear interior. *J. Cell Biol.* 144:839–855.

Stutz, F., and M. Rosbash. 1998. Nuclear RNA export. *Genes Dev.* 12:3303–3319.

Sun, X., A.T. Alzhanova-Ericsson, N. Visa, Y. Aissouni, J. Zhao, and B. Daneholt. 1998. The hrp23 protein in the balbiani ring pre-mRNP particles is released just before or at the binding of the particles to the nuclear pore complex. *J. Cell Biol.* 142:1181–1193.

Visa, N., E. Izaurralde, J. Ferreira, B. Daneholt, and I.W. Mattaj. 1996a. A nuclear cap-binding complex binds Balbiani ring pre-mRNA cotranscriptionally and accompanies the ribonucleoprotein particle during nuclear export. *J. Cell Biol.* 133:5–14.

Visa, N., A.T. Alzhanova-Ericsson, X. Sun, E. Kiseleva, B. Bjorkroth, T. Wurtz, and B. Daneholt. 1996b. A pre-mRNA-binding protein accompanies the RNA from the gene through the nuclear pores and into polysomes. *Cell.* 84:253–264.

von Besser, H., P. Schnabel, C. Wieland, E. Fritz, R. Stanewsky, and H. Saumweber. 1990. The puff-specific *Drosophila* protein Bj6, encoded by the gene no-on transient A, shows homology to RNA-binding proteins. *Chromosoma.* 100:37–47.

Wang, J., L.G. Cao, Y.L. Wang, and T. Pederson. 1991. Localization of premessenger RNA at discrete nuclear sites. *Proc. Natl. Acad. Sci. USA.* 88: 7391–7395.

Wieslander, L. 1994. The Balbiani ring multigene family: coding repetitive sequences and evolution of a tissue-specific cell function. *Prog. Nucleic Acid Res. Mol. Biol.* 48:275–313.

Wurtz, T., E. Kiseleva, G. Nacheva, A. Alzhanova-Ericson, A. Rosen, and B. Daneholt. 1996. Identification of two RNA-binding proteins in Balbiani ring premessenger ribonucleoprotein granules and presence of these proteins in specific subsets of heterogeneous nuclear ribonucleoprotein particles. *Mol. Cel. Biol.* 16:1425–1435.

Wyss, C. 1982. *Chironomus tentans* epithelial cell lines sensitive to ecdysteroids, juvenile hormone, insulin and heat shock. *Exp. Cell Res.* 139:309–319.

Xing, Y., C.V. Johnson, J.P.T. Moen, J.A. McNeil, and J.B. Lawrence. 1995. Nonrandom gene organization: structural arrangements of specific pre-mRNA transcription and splicing with SC-35 domains. *J. Cell Biol.* 131: 1635–1647.

Zachar, Z., J. Kramer, I.P. Mims, and P.M. Bingham. 1993. Evidence for channeled diffusion of pre-mRNAs during nuclear RNA transport in metazoans. *J. Cell Biol.* 121:729–742.

Zimowska, G., J.P. Aris, and M.R. Paddy. 1997. A *Drosophila* Tpr homolog is localized both in the extrachromosomal channel network and to nuclear pore complexes. *J. Cell Sci.* 110:927–944.